

Picophytoplankton as tracers of environmental forcing in a tropical monsoonal bay

Smita Mitbavkar · Jagadish S Patil · Rajaneesh KM

Council of Scientific and Industrial Research, National Institute of Oceanography,
Dona Paula, Goa 403 004, India.

Corresponding author: Smita Mitbavkar

E-mail: mitbavkars@nio.org

Tel. (+91) 832 2450376

Abstract In order to better understand the picophytoplankton (PP) dynamics in tropical monsoon influenced coastal regions, samples were collected daily (June-September'08:monsoon, December'08:post-monsoon and April'09:pre-monsoon) from a fixed station in Dona Paula Bay, India. Eight PP abundance peaks comprising *Prochlorococcus*-like cells, picoeukaryotes and three groups of *Synechococcus* occurred. Lowering solar radiation, salinity and water transparency as a consequence of precipitation, whereas stabilized waters during precipitation breaks/non-monsoon periods influenced the chlorophyll biomass and PP abundance negatively and positively, respectively. Responses to environmental conditions differed with PP groups wherein presence of *Synechococcus*-PEI (phycoerythrin) throughout the year suggested its ability to tolerate salinity and temperature variations and low light conditions. *Synechococcus*-PEII appearance towards monsoon end and non-monsoon during high water transparency suggests its tidal advection from offshore waters. Dominance of *Synechococcus*-PC (phycocyanin) at intermediate salinities under low water transparency during MON and high salinities in PrM coinciding with high nitrate concentrations implies a greater influence of light quality or nutrients. Cyanobacteria and not picoeukaryotes were the dominant picophytoplankton in terms of numbers as well as biomass. This study suggests that PP could be used as tracers of environmental forcing driven by tides and freshwater influx and also highlights the importance of high frequency samplings in dynamic coastal regions through which transient responses can be captured.

Keywords: Picophytoplankton; tracers; environmental forcing; daily observations; monsoon; tropical bay

Introduction

Phytoplankton dynamics are controlled by physical (e.g. light, temperature, water motion), chemical (e.g. salinity, nutrients) and biological (e.g. predation, viral attack, eukaryotic parasites) factors [1, 2]. Variations of these factors over different time frames i.e., diel, daily, fortnightly, monthly, seasonally, drives the temporal variations of biomass and activity within the microbial food web [3]. The number and timing of peaks detected in the time series of phytoplankton biomass largely depend on the sampling frequency employed [4, 5]. Sporadic blooms of plankton can be missed due to low frequency samplings leading to erroneous results [6]. Although extensive plankton studies have been conducted in the temperate waters on various time scales [7] these cannot be a representative for the comparatively less investigated tropical ecosystems [8] due to the latitudinal differences in environmental forcing.

In the tropics, which are influenced by the South-West monsoon (June to September), the hydrography of coastal regions such as bays and estuaries is controlled by the freshwater influx from the land drainage and the flow from the upstream end of the estuary more than the tidal flow during monsoon. Conversely, during the non-monsoon period, as the freshwater influx dies down, the hydrography is controlled by the tidal flow [9]. During the monsoon season, the precipitation exhibits variations in intensity as well as breaks in rainfall. During this season, depending on the pattern of rainfall, the hydrographical features and environmental factors also vary correspondingly [10]. This consequently influences the biological communities such as planktons prevailing in these water bodies [11, 12]. In such a scenario, continuous observations on a daily basis at longer time scales would be pertinent to capture the responses of phytoplankton to short-term hydrographic variability which would otherwise be missed in low frequency samplings.

Picophytoplankton (PP) is the smallest size group (0.2 to 3 μm) of phytoplankton which form the base of the microbial food web. Few studies on PP community variations have been conducted on monthly and seasonal scales in the Western Arabian Sea [8, 13, 14] and the coastal regions of the Eastern Arabian Sea [15, 16, 17]. In the present study, for the first time, we were able to discern the daily responses of PP to the changing environmental conditions during MON and non-MON in a tropical bay of the Eastern Arabian Sea. Earlier studies on PP have been conducted on a daily scale in the open ocean regions [1, 5, 18], coastal regions [2, 7] and oligotrophic regions such as the coral lagoons [19] but not in monsoon influenced coastal ecosystems.

Our previous studies in a tropical estuary have shown temporal variations in PP community on monthly and seasonal scales [17]. However, there is no information on their behavior on shorter time scales in tropical coastal regions. In this study, we examined the PP community on daily time scales for three seasons from the Dona Paula Bay. This is a semi-enclosed bay that opens into the Arabian Sea and located at the mouth of the Zuari estuary with the periodic freshwater inflow during the monsoon controlling its hydrography [9]. Unlike many other estuaries in the world, the Zuari estuary is unique in terms of the annual cycle of salinity

distribution associated with the south west monsoon [20]. The complex hydrodynamics of this area makes it quite different from the other coastal areas where the water column is homogeneous most of the year.

We hypothesized that the intra-seasonal and inter-seasonal hydrographic conditions in the bay will be reflected in the PP community structure. Our aim was to assess the temporal variations of PP community structure in a tropical coastal ecosystem influenced by the SW monsoon and identify the environmental factors that control the variability on daily and seasonal time scales. Contribution of PP to the total phytoplankton biomass was also examined.

Material and Methods

Study area

Sampling was done in the Dona Paula Bay at a fixed location ($15^{\circ} 27.5^{\circ}$ N; $73^{\circ} 48^{\circ}$ E; average depth 3 m), Goa, along the west coast of India (Fig. 1). In the bay, this study site is situated at the head of the monsoonal estuary and is influenced by high annual freshwater runoff as well as tides depending on the seasons. These characteristics make the environment in the bay unique to address the plankton responses to environmental perturbations driven by monsoons. This locality experiences three seasons: the pre-monsoon (February-May; PrM), the South-West monsoon (June-September; MON) and the post-monsoon (October-January; PM). The highest wind speed is experienced during the monsoon season along with an increased suspended load in the overlying waters. The wind speed is lowest in the PM season, and increases with the beginning of the pre-monsoon season. The tides are semidiurnal with an average spring tide range of ~ 2.3 m [21] and neap tide range of ~ 0.7 m. The wave heights are > 1.5 m during June to August [22]. Daily tidal amplitudes for the study period were calculated from the tide table.

Sampling strategy

Surface water samples were collected daily between 11:00 to 12:00 h with the help of a bucket from June 1, 2008 to September 30, 2008, to cover the MON season, followed by PM sampling from December 1 to 31, 2008 and PrM sampling from April 1 to 30. The time was fixed to avoid the complexity of diurnal changes in the biogeochemical properties while comparing the data. Temperature and secchi disk depth for water transparency were noted every day at the study site. Salinity measurements were done with an autosal. Meteorological data of precipitation and solar radiation data for the study period was obtained from the Indian Meteorological Department (IMD).

Water samples for nutrient analysis were collected once in two days. Nitrate (NO_3^-), nitrite (NO_2^-), phosphate (PO_4^{3-}), ammonium (NH_4^+) and silicate (SiO_4^{4-}) concentrations were determined spectrophotometrically following standard procedures [23]. Water samples for size fractionated chlorophyll *a* (chl *a*) analysis were

filtered through $< 3 \mu\text{m}$ millipore filter paper and *in-vivo* fluorometric measurement of chl *a* using Turner fluorometer (Triology) from the unfiltered sample and from $< 3 \mu\text{m}$ fraction was done to estimate the relative contribution of PP to total photosynthetic biomass. Total chl *a* concentration was also estimated through spectrofluorometric method [23] by filtering 250 mL of seawater through Whatman GF/F glass-fiber filters and measuring the concentration after extraction in 90% acetone for 24 h.

Flow cytometric analysis

Samples for PP analysis were collected in 2 mL cryovials and preserved in paraformaldehyde (0.2% final concentration), flash frozen in liquid nitrogen and subsequently stored at -80°C until analysis. PP were analyzed with a BD FACS AriaTM II flow cytometer equipped with a blue and red laser excited at 488 nm and 633 nm, respectively. The forward light scatter and right angle light scatter (RALS) signals were collected along with the orange fluorescence from phycoerythrin, red fluorescence from chlorophyll and red fluorescence from phycocyanin. The blue and red lasers are used to discriminate the red fluorescence produced by chlorophyll and phycocyanin pigments, respectively. Fluorescent beads ($2 \mu\text{m}$ for PP “Fluoresbrite”, polysciences) were used as internal standards and for calibration of the above parameters. Data obtained was processed with the BD FACS Diva (Version 6.2) software. PP groups were discriminated and enumerated according to their specific autofluorescence properties and light scatter differences.

The PP community comprised four groups which were distinguished based on the autofluorescence from the cellular pigments and the light scatter signals (Fig. 2). The group of cells with the smallest RALS and low red fluorescence were identified as *Prochlorococcus*-like cells (*PRO*-like cells) and the group with the largest RALS and high red fluorescence were considered as picoeukaryotes (PEUK). Two groups of *Synechococcus* (*SYN*) were discriminated based on the orange and red fluorescence from the phycoerythrin and phycocyanin pigments, respectively. The former was designated as *SYN*-PE and the latter as *SYN*-PC. The *SYN*-PE group comprised two sub-groups based on the intensity of the orange fluorescence wherein one possessed lower fluorescence (*SYN*-PEI) than the other (*SYN*-PEII).

Data analyses

Cross correlation analyses were performed in order to assess the influence of rainfall on salinity and solar radiation and also the relationship of chl biomass and PP groups cell abundance with environmental parameters such as salinity, temperature, water transparency and solar radiation. Cross correlation analyses were performed at an interval of 1 d ranging from 7 d previous through 7 d forward in time with the Statistica software. Linear regression was performed to assess the influence of nutrient concentrations on the chl biomass and PP groups cell abundance.

The carbon biomass for the different PP groups was estimated by the calibration method of [24]. In short, the RALS data of each PP group were converted to cell diameter which was later used to estimate the biovolume using the equation, $V = \frac{4}{3} \pi r^3$ (d3), assuming the PP cells to be spherical. Biovolume to carbon conversion

factors of 254 fg C μm^{-3} , 240 fg C μm^{-3} and 239 fg C μm^{-3} for *Synechococcus* [25], *Prochlorococcus*-like cells and picoeukaryotes [24], respectively were used.

Results

Meteorology and hydrography

Solar radiation fluctuated from low (4.9 mw cm^{-2}) to high (67.3 mw cm^{-2}) levels during MON due to cloud cover whereas during non-MON, it was stable (36 to 65 mw cm^{-2} ; Fig. 3A). MON started from June 2 with the highest rainfall of 137 mm on June 8 and the second highest of 130 mm on August 10. Higher rainfall was recorded between June 7 to 13, July 17 to 18, August 6 to 13 and September 11 to 13. Precipitation was below 50 mm on most occasions (Fig. 3B).

During MON, water transparency was below 100 cm from June to August and thereafter it started increasing and was highest towards the beginning of September (265 cm) when break in MON prevailed. During the non-MON it was above 100 cm and ranged up to 257 cm in PM (Fig. 3C). During PM and PrM, water transparency was comparatively higher. During MON, water temperature gradually declined from June to mid-August subsequent to which it increased up to September end. Water temperature ranged from 25.8 to 30.5°C with the highest recorded in June and lowest in August (Fig. 3D). In December, water temperature was 30°C and in April the highest annual range was recorded (31 to 32.5°C). In June when the highest rainfall was recorded, surface salinity of the bay was > 30 (Fig. 3E). This could be due to the delay in freshwater inflow from the upstream end of the estuary. Salinity started to decline only after June 12. Thereafter oscillations were observed in the salinity profile ranging from 2 to 35.4 with the lowest on August 19 and highest on August 31. Salinity was below 5 and 10 on some occasions in August and September when peaks in precipitation were recorded. In the beginning of PM, surface salinity was 28 which gradually increased to 35, with the same trend in PrM.

Nutrient concentrations

During MON, NO_3^- , NO_2^- , NH_4^+ , PO_4^{3-} and SiO_4^{4-} concentrations varied between 0.07 to 22.5 μM , 0.02 to 0.97 μM , 0.1 to 24.6 μM , 0.39 to 3.96 μM and 20 to 80 μM , respectively (Fig. 4A-E). Nutrient concentrations were high till mid-August. From August 22 to September 10, nutrient concentrations declined when surface salinity increased from ~ 20 to 30 with low rainfall. Highest NO_3^- concentrations (22.51 μM) were recorded on 12 June when the salinity started to decline indicating the influence of freshwater influx. On this day, peak in NO_2^- (0.46 μM) was also observed. NO_2^- concentrations were highest on 11 August (0.97 μM). Similarly, NH_4^+ concentration was higher from June to mid-August with a peak on 11 August (24.6 μM). PO_4^{3-} was highest on 9 June (3.96 μM). In PM and PrM, nutrient concentrations were comparatively lower. In PM, NO_3^- , NO_2^- and PO_4^{3-} concentrations varied between 0.78 to 4.76 μM , 0.01 to 0.09 μM and 0.15 to 1.19 μM , respectively. In PrM, NO_3^- , NO_2^- , NH_4^+ and PO_4^{3-} concentrations varied between 0.13 to 9.13, 0.01 to 0.06, 0.27 to 8.83 and 0.32 to 1.12 μM , respectively. SiO_4^{4-} concentration was below 20 μM during both seasons.

Chlorophyll *a* concentrations

Bulk chl *a* concentrations in the MON, PM and PrM ranged from 0.27 to 8.97, 0.44 to 2.14 and 0.64 to 2.67 $\mu\text{g L}^{-1}$. Concentrations peaked from 25-27 June, 20-21 August and 2-4 September (Fig. 5A). These periods followed the peaks in nutrient concentrations and coincided with breaks in MON. Linear regression analysis between total chl *a* concentration and bulk chl *a* fluorescence (Fig. 5B) measured *in vivo* showed a significant positive relation ($r^2 = 0.685$, $P < 0.001$) which implies a reliable co-relation between the two methods of chl *a* analysis. The $< 3 \mu\text{m}$ chl *a* fluorescence measured *in vivo* showed highest peak in the beginning of June (Fig. 5C). In MON, other peaks were observed at the end of June, July, August and September. During PM and PrM, fluorescence values were higher than in MON. During MON, contribution of PP to the total chl *a* biomass ranged from 0.4-33.0% with the highest contribution on September 25 (Fig. 5D). This contribution ranged from 7-49% in PM and 6-40% in PrM.

Picophytoplankton abundance

During the study period, eight major peaks in PP cell abundance were observed in the Dona Paula Bay (Fig. 6A-F) with four during MON (between June 1 and June 3, July 9 and July 28, July 9 and July 28, September 17 and September 26) and two each during the PM (on December 5 and December 13) and PrM (between April 9 and 18, April 21 and 29). The first PP abundance peak was dominated by *SYN-PC* (10.2×10^4 cells mL^{-1} , 76% of total PP abundance). This peak was reflected in the $< 3 \mu\text{m}$ chl *a* concentration. The bulk photosynthetic biomass was also high during this period. After June 3, with the onset of heavy precipitation, PP cell abundance declined markedly. An increase in chl *a* concentration was observed between June 19 and June 28. During this period only *SYN-PEI* abundance was higher (1.0×10^4 cells mL^{-1} , 76% of total PP abundance). The second peak in PP abundance was represented by *SYN-PEI*, *SYN-PC*, *PRO*-like cells and *PEUK*. *SYN-PEI* (4.1×10^4 cells mL^{-1} , 89% of total PP abundance) and *PRO*-like cells (2.5×10^4 cells mL^{-1} , 39% of total PP abundance) dominated the PP community. During this period comparatively higher chl *a* concentrations were observed. Subsequently, the PP cell abundance declined ($< 1.5 \times 10^4$ cells mL^{-1}) up to August 17. The third peak in PP abundance was represented by *SYN-PEI* (28%), *PEUK* (27%), *SYN-PC* (17%) and *PRO*-like cells (26%) except *SYN-PEII* (0.25%). The bulk chl *a* biomass peaked first followed by that of $< 3 \mu\text{m}$ chl *a* peak and a second peak in bulk chl. Another peak in bulk chl *a* was observed on September 2. Although no peak in $< 3 \mu\text{m}$ chl *a* was observed but *SYN-PEI* and *PEUK* were abundant during this period. After this, from September 7 to September 16, the PP abundance declined (1.8×10^4 cells mL^{-1}). The fourth PP abundance peak was represented by all PP groups and dominated by *PRO*-like cells (4.8×10^4 cells mL^{-1} , 47%) followed by *SYN-PEI* (2.0×10^4 cells mL^{-1} , 25%) and *SYN-PC* (2.0×10^4 cells mL^{-1} , 21%). The fifth and sixth peaks during PM were dominated by *SYN-PEI* (3.1×10^4 cells mL^{-1} , 66%; 4.3×10^4 cells mL^{-1} , 83%, respectively). During the first half of December, peaks in contribution of $< 3 \mu\text{m}$ chl *a* to bulk chl *a* were observed, which were higher than that in MON. The seventh and eight PP abundance peaks during the PrM

were dominated by *SYN*-PE (78% and 55%, respectively). Increased contribution of $< 3 \mu\text{m}$ chl *a* which coincided with increase in *SYN*-PC abundance (4.8×10^4 cells mL^{-1} , 64%) was observed during the last peak.

Relationship between environmental parameters

Cross correlation analysis showed that salinity was negatively correlated with rainfall at zero time lag through 7 d in forward time with the largest correlation after 5 d of rainfall (Fig. 7A). Solar radiation was negatively correlated with rainfall from 7 d in reverse time through 4 d in forward time with highest correlation from 1 d in reverse time and at zero time lag. Surface water temperature was negatively correlated from 3 d in reverse time through 5 d in forward time with highest correlation at zero time lag (Fig. 7A). Water transparency was positively correlated with salinity during MON at zero time lag through 5 d in forward time with the largest correlation after 3 d (Fig. 7A). During non-MON water transparency and salinity did not show any significant relationship (Fig. 8A and 9A). Amongst the nutrients, SiO_4^{4-} concentrations negatively correlated with salinity ($r^2 = 0.5$, $P < 0.001$) during MON whereas NO_3^- ($r^2 = 0.57$, $P < 0.02$) and SiO_4^{4-} ($r^2 = 0.46$, $P < 0.05$) negatively correlated with salinity during PrM.

Relationship between chlorophyll biomass and environmental parameters

Bulk chlorophyll a

During MON, bulk chl *a* correlated positively with salinity (from 7 d in reverse time through 5 d in forward time), temperature (from 3 d in reverse time and at zero time lag), water transparency (from 5 d in reverse time through 5 d in forward time) and solar radiation (at zero time lag through 7 d in forward time) (Fig. 7B). During PM, bulk chl *a* was negatively correlated with salinity (at zero day lag through 3 d in forward time), temperature (from 4 to 5 d in forward time), water transparency (from 5 d in reverse time and 1 to 3 d in forward time) (Fig. 8B). During PrM, bulk chl *a* was negatively correlated with water transparency (from 4 d in reverse time and at zero time lag) (Fig. 9B). During MON total chl *a* was negatively correlated with NO_3^- ($r^2 = 0.29$, $P < 0.001$), PO_4^{-3} ($r^2 = 0.1$, $P < 0.01$) and SiO_4^{4-} ($r^2 = 0.14$, $P < 0.02$).

$< 3 \mu\text{m}$ chlorophyll *a*

During MON, $< 3 \mu\text{m}$ chl *a* correlated positively (from 7 d in reverse time and at zero time lag), temperature (from 3 d in reverse time through 5 d in forward time), water transparency (from 2 d in reverse time through 4 d in forward time) and solar radiation (from 2 d in reverse time through 4 d in forward time) (Fig. 7C). During PM, $< 3 \mu\text{m}$ chl *a* was negatively correlated with salinity (at zero day lag through 1 d in forward time) and positively correlated with temperature (from 2 d in forward time) (Fig. 8C). During PrM, $< 3 \mu\text{m}$ chl *a* did not show any significant relation with any of these parameters (Fig. 9C). During MON ($r^2 = 0.16$, $P < 0.02$) and PM ($r^2 = 0.37$, $P < 0.05$), the $< 3 \mu\text{m}$ chl *a* was negatively correlated with PO_4^{-3} . In the PrM, $< 3 \mu\text{m}$ chl *a* showed a positive correlation with NO_3^- ($r^2 = 0.8$, $P < 0.01$) and SiO_4^{4-} ($r^2 = 0.72$, $P < 0.01$).

Relationship between abundance of picophytoplankton groups and environmental parameters

Synechococcus-PEI (SYN-PEI)

During MON, this PP group correlated positively with salinity (at zero time lag) and temperature (zero time lag through 7 d in forward time), negatively with water transparency (from 3 d in reverse time through 1 d in forward time) and no significant relation with solar radiation (Fig. 7D). During PM, *SYN-PEI* was not significantly correlated with these environmental parameters (Fig. 8D). During PrM, this group was correlated negatively with water transparency (from 1 to 2 d in reverse time from 2 d in forward time) and positively with solar radiation (from 6 d in forward time) (Fig. 9D). *SYN-PEI* was negatively correlated with NH_4^+ ($r^2 = 0.12$, $P < 0.05$).

Synechococcus-PEII (SYN-PEII)

During MON, this group correlated positively with salinity (from 4 d in reverse time through 2 d in forward time), temperature (from 2 d in reverse time and at zero time lag), water transparency (5 d in reverse time through 7 d in forward time) and solar radiation (from 2 to 7 d in forward time) (Fig. 7E). During PM, this group was positively correlated (after 3 d in forward time) only with salinity (Fig. 8E). During PrM, this group was positively correlated with temperature (after 7 d) and water transparency (at zero time lag) (Fig. 9E). During MON, *SYN-PEII* was negatively correlated with NO_3^- ($r^2 = 0.12$, $P < 0.05$) and PO_4^{3-} ($r^2 = 0.12$, $P < 0.05$).

Synechococcus-PC (SYN-PC)

During MON, this group correlated positively with salinity in reverse time (from 2 to 7 d) and negatively in forward time (from 5 to 6 d), positively with temperature (from 6 d in reverse time through 4 d in forward time) and solar radiation (at zero time lag through 2 d in forward time) and negatively with water transparency (from 2 to 7 d in forward time) (Fig. 7F). During PM, this group was positively correlated with salinity (after 3 d in forward time) (Fig. 8F). During PrM, this group was positively correlated with solar radiation (from 2 d in forward time) and negatively with water transparency (from 4 d in reverse time through 1 d in forward time) (Fig. 9F). One occasion of higher nutrient concentration coincided with lower water transparency during PrM. During this period, *SYN-PC* was positively correlated with NO_3^- ($r^2 = 0.43$, $P < 0.05$).

Prochlorococcus-like cells (PRO-like)

During MON this group correlated negatively with salinity (from 1 d in reverse time through 7 d in forward time) and water transparency (from 5 to 7 d in forward time) (Fig. 7G). During PM, this group was positively correlated (after 2 d in reverse time) only with salinity (Fig. 8G). During PrM, this group was negatively correlated with water transparency (from 4 to 5 d in reverse time) and positively correlated (from 1 d in reverse time) and negatively correlated (from 6 d in forward time) with solar radiation (Fig. 9G). *PRO*-like cells negatively correlated with NH_4^+ during MON ($r^2 = 0.24$, $P < 0.01$).

Picoeukaryotes (PEUK) During MON this group correlated positively with salinity (from 4 to 5 d in forward time) and water transparency (from 3 to 4 d in reverse time) and negatively (from 3 to 4 d in reverse time and from 1d in forward time) with temperature (Fig. 7H). During PM, this group was positively correlated with salinity (from 2 to 3 d in reverse time) (Fig. 8H). During PrM, this group was positively correlated with temperature (from 3 to 4 d in forward time) and negatively correlated with solar radiation (from 1 d in reverse time) (Fig. 9H). PEUK were negatively correlated with NH_4^+ during MON ($r^2 = 0.12$, $P < 0.05$).

Contribution of each group to total picophytoplankton carbon biomass

Cyanobacteria (*SYN* and *PRO*-like cells) were the dominant PP in terms of numbers (on an average 90% in MON and > 95% in non-MON period) as well as biomass (on an average 87%, 96% and 95% of the total PP biomass in the MON, PM, PrM, respectively). The remaining PP biomass was accounted for by PEUK. The total PP biomass during MON ranged from 0.3 to 24 $\mu\text{g C L}^{-1}$ whereas in the non-MON period ranged from 28 to 570 $\mu\text{g C L}^{-1}$ in December and 42 to 914 $\mu\text{g C L}^{-1}$ in April. On an average, *SYN*-PC was the major contributor to the total PP biomass in MON (37%) followed by *SYN*-PE-I (25%), *PRO*-like cells (23%) and PEUK (14%). In December, 66% was contributed by *SYN*-PEI whereas *SYN*-PC contributed 17% followed by *PRO*-like cells (6%) and PEUK (4%). In April, 47% was contributed by *SYN*-PC followed by *SYN*-PEI (31%), *PRO*-like cells (13%) and PEUK (5%). *SYN*-PEII was the least contributor throughout the sampling period.

Discussion

Temporal and spatial variation of the plankton community in coastal waters is governed by a variety of physical, chemical and biological processes such as advection, establishment of weather fronts, stratification, vertical mixing, water temperature, light, nutrient supply, and predation pressure [26] which are in turn driven by daily changes in air temperature, solar radiation, wind and rainfall associated with passage of meteorological fronts [27]. In the tropics, precipitation during MON is a characteristic meteorological feature which governs the seasonal hydrography and environmental cycle [10]. Depending on the location, the type of environmental forcing varies. In the Western Arabian Sea, the main environmental forcing is upwelling and convective mixing responsible for delivering nutrients to the surface waters [13]. In the present study area in the eastern Arabian Sea, a tropical bay along the west coast of India, the main environmental forcing during the SW-MON is the influx of freshwater from the upstream end of the Zuari estuary due to precipitation, which brings about salinity variations in the bay seasonally and also fertilizes the bay waters [10] whereas during the non-MON seasons it is replaced by the tidal influence.

Picophytoplankton groups

At a coastal station off Oman in the western Arabian Sea, *SYN* abundance ranged up to 5.0×10^4 cells mL^{-1} during the SW-MON [14] which was similar to that observed in this study, although environmental forcing are different. In the former case upwelling prevails whereas in this study it was the influx of freshwater. Along with abundance, the sub-groups observed at the two sites were also comparable. In the North-Western Arabian

Sea, two different types of *SYN* were reported which were defined by the ratios of their phycoerythrin chromophore composition i.e., phycourobilin (PUB) and phycoerythrobilin (PEB) and distinguished based on their fluorescence signatures through flow cytometry [13]. They reported increased abundances of “bright” *SYN* subpopulation offshore, whereas a “dim” subpopulation tended to be higher at coastal stations. So in the present study, *SYN*-PEI with a lower phycoerythrin fluorescence and *SYN*-PEII with a higher fluorescence observed during all the seasons and only during the non-MON seasons, respectively, suggests that the former could be the “dim” and latter the “bright” *SYN* subpopulation. During SW-MON, the dominant form of PE was the low PUB:PEB pigment type in coastal regions and high PUB:PEB pigment type offshore with mixtures of pigment types during NE-MON and fall intermonsoon [13] which corroborated with our findings. High PUB/PEB cyanobacteria are often present in oligotrophic open-ocean ecosystems, while the low PUB/PEB clones are mainly encountered in nutrient-rich environments [28]. Part of the PUB/PEB changes could be ascribed to environmental changes particularly light intensity since some *SYN* clones are capable of changing their phycoerythrin spectral properties in accordance with light conditions [29]. PUB rich *SYN* appear to be dominant across the open ocean because of their enhanced ability to absorb blue light [28]. This could also be a reason for their absence during the MON and presence during non-MON in the bay which is supported by the cross correlation analysis wherein high water transparency favours this group.

SYN-PC group was not reported from the earlier studies in the coastal stations of the North-Western Arabian Sea. Studies in the oceanic systems have reported the presence of only PE-containing *SYN* [30]. In the coastal and estuarine systems there are some studies that have reported both, the PC and PE containing *SYN* wherein the PE-rich *SYN* use phycoerythrin and PC-rich ones phycocyanin as major light-harvesting pigments [31, 32]. The average PC:PE ratio of 1.11, 0.83 and 1.10 during the MON, PM and PrM (Fig. 10) highlights the importance of PC cyanobacteria in coastal systems. A detailed comparison of such studies in estuarine systems by [33] shows that some studies have either used blue light excitation only, in which case total cyanobacterial numbers are likely to be underestimated, or have used both green and blue excitation light but do not distinguish between PE and PC cyanobacteria types. In this study this differentiation between the two groups of *SYN* depending on their pigment types was made possible through the use of blue and red lasers of flow cytometry.

Although, *Prochlorococcus* is a group that is known to occur in high abundance in the oceanic regions, this group is reported from the coastal waters of the Western Arabian Sea during the SW-MON [8, 13, 14, 34] with cell concentrations (5×10^4 cells mL⁻¹) similar to that recorded for the *PRO*-like cells in the present study. In the present study, the highest abundance of this group was recorded between a salinity range of 5 to 20. Their presence in coastal waters which are being reported in the recent years is still speculative whether it is brought from the open oceans or they are actually growing in these waters [35].

Environmental forcing on chlorophyll a

At the beginning of sampling during the MON, due to low precipitation, solar radiation was high and the water column was stable with high water temperature, salinity and water transparency. Earlier reports have shown that PP thrives in such conditions in coastal regions [16,17,36]. Similarly, during the present study, peak in PP abundance was observed. These observations were corroborated by the substantially high contribution of $< 3 \mu\text{m}$ chl *a* to the bulk chl *a* biomass, which also peaked during this period.

Subsequently, with the onset of rainfall accompanied by strong, westerly to south-westerly winds with a speed of $4\text{-}7 \text{ m s}^{-1}$ [10], which tend to strengthen the currents towards the estuary head, the stability of the water column was disturbed along with a change in meteorological and environmental conditions. Cross correlation analysis showed that solar radiation, temperature and salinity started declining on the day of rainfall with maximum reduction of first two parameters on the same day and surface water salinity after 5 d of rainfall suggesting a lag in entry of freshwater from upstream. The environmental changes occurring on the day the rainfall started could be attributed to freshwater addition directly from precipitation and surrounding land runoff. The high freshwater runoff due to rainfall resulted in high concentrations of nutrients in the bay similar to that reported in other studies [10, 37]. However, the decline in chlorophyll biomass during this period implied that more than nutrients, the other unfavourable environmental conditions had an overriding effect on the phytoplankton growth. This decline in biomass persisted till the environmental conditions started improving.

The SW-MON season is characterized by transient periods of absence or lowered precipitation when the freshwater runoff subsides temporarily and the meteorological and hydrographical conditions return back to normal thereby increasing the stability of the water column [10]. The increased surface salinity during this period also implies a temporary shift in the environmental forcing from freshwater influx to tidal flow in regulating the bay hydrography which may also facilitate entry of cells into the bay from coastal waters. During this period, the nutrient concentrations were high as a result of the accumulation from the freshwater runoff and non-utilisation by the phytoplankton. This along with the increased water transparency, temperature, salinity and solar radiation triggered an increase in phytoplankton biomass as seen from the positive correlation. Water transparency was positively correlated with salinity. Bulk and $< 3 \mu\text{m}$ chl *a* were maximum on the day of salinity increase up to 5 d and 3 d, respectively and decreased 7 d later. During this period, the decreasing trend of nutrient concentrations corresponding with increasing bulk chl *a* concentrations as seen from the negative correlation between the two suggests nutrient consumption by the nano and microphytoplankton [11,38,39]. The subsequent fall in bulk chl *a* biomass followed by a peak in $< 3 \mu\text{m}$ chl *a* biomass although at lower levels to that of bulk chl *a* as seen from the negative correlation with phosphate suggests that PP succeeds the higher phytoplankton community. This is in agreement with the previous studies which show that PP are at an advantage under low nutrient concentrations [40]. The following second peak of bulk chl *a* suggests that higher phytoplankton representing groups that can sustain at low nutrient concentrations dominate during this period. This also included PP groups such as *SYN-PEI* and

PEUK. Cross correlation analysis shows that $< 3 \mu\text{m chl } a$ and bulk chl a concentrations increased at zero time lag in water transparency and solar radiation and continued for 4 d and 5 d later, respectively. During this period a species succession was occurring depending on the nutrient availability/requirement wherein the phytoplankton diversity was represented by different size groups (Patil and Anil, unpublished data). Previous studies in this bay have reported a change in the microphytoplankton composition from a *Skeletonema* and *Fragilariopsis* dominated bloom during precipitation period to a mixed species bloom of large diatoms and dinoflagellates [11] which are adapted to high saline and nutrient limited conditions during MON breaks.

During PM and PrM, when precipitation was nil and hence no freshwater influx, the bay hydrography is governed by tides and the water column is comparatively stable with higher solar radiation, water temperature, transparency and salinity [10] and lower nutrient concentrations. This is reflected in the comparatively lower bulk chl a biomass. However, the $< 3 \mu\text{m chl } a$ biomass was almost similar to that observed in the MON with higher intermittent peaks leading to a comparatively higher contribution to the bulk chl a biomass. This suggests that the environmental factors leading to a stable water column exert a greater positive influence on the growth of PP than the nutrient concentrations as compared to the higher phytoplankton which require high nutrient concentrations for their growth [39]. This is substantiated by the negative correlation of PP with PO_4^{-3} during PM which suggests that $< 3 \mu\text{m chl } a$ biomass increases when the PO_4^{-3} concentrations are substantially low. i.e., when the larger phytoplankton are not capable of growing due to low nutrient concentrations. This was also observed during MON. In other words, larger phytoplankton were PO_4^{-3} limited. During non-MON due to lack of freshwater influx the source of nutrients is limited to benthic resuspension due to vertical mixing [37]. In the PrM, one occasion of higher nutrient concentration coincided with lower water temperature, salinity and transparency which could probably be due to benthic resuspension. This was substantiated by a negative correlation of NO_3^- and SiO_4^{4-} with salinity. Although the relation with transparency was negative it was not significant. Corresponding increase in bulk chl a biomass and a higher contribution by $< 3 \mu\text{m chl } a$ suggests a response from phytoplankton species that were limited by these nutrients [11].

Influence of environmental forcing on the PP groups

During the MON season the freshwater influx can reach to the extent of flushing out most of the saline water from the bay [9] as was observed in August when the surface salinity was lowered to 2. The impact of such physical forcing was reflected in the lowered PP cell abundance and may be ascribed to the dilution effect of seawater by freshwater or, equally the elimination of some marine species by osmotic stress or growth disturbance due to the negative influence of meteorological and hydrographical conditions. Such physical forcing can also bring some groups from the upstream end of the estuary into the bay. Similar to earlier reports, increase in rainfall resulted in higher concentrations of SiO_4^{4-} and NH_4^+ in the bay waters as reported earlier [37]. PP are known to be abundant in nutrient poor waters but also respond to nutrient enrichment in stable water conditions [40]. In the present study, high nutrient concentrations did not have a positive

influence on the growth of PP which suggests an overriding negative effect of the other prevailing unfavourable conditions.

Amongst the PP, group wise differences in responses to environmental conditions were observed. The presence of *SYN-PEI* throughout the sampling period albeit at lower numbers during precipitation and higher numbers during breaks in precipitation and non-MON suggests that this group is a native of the bay. This conjecture is supported by its positive correlation with temperature and salinity which implies a positive influence of water stability during MON. Also, the negative relation with water transparency along with absence of significant correlation with solar radiation suggests that this group is able to survive even under low light conditions. Its ability to grow under low water transparency was also observed during the non-MON which coincided with an increase in nutrient concentrations in the surface waters. These abilities probably were responsible for its presence throughout the year.

In comparison to *SYN-PEI*, *SYN-PEII* appeared only towards the end of the MON season and persisted throughout the non-MON season. Cross correlation analysis showed that *SYN-PEII* group was positively controlled by water transparency wherein during MON its abundance was most significantly influenced within 1 d. Its presence at the beginning of sampling when the precipitation was low and solar radiation, temperature and salinity were high, followed by its disappearance and sudden appearance at the end of MON when the precipitation was reducing with a consequent change in the environmental forcing from fresh water runoff to tides, suggests that probably the original source of these cells is the offshore waters from where they are brought into the bay during the high tide (Fig.11). In coastal regions, tides are also known to influence the phytoplankton abundance [41]. Appearance of this group in the bay waters can be a marker of the initiation of the entry of offshore waters into the bay which is reflected in the increased salinity. This conjecture is supported by the positive correlation with temperature, salinity and solar radiation in opposition to the negative relation of *SYN-PEI* with water transparency. Also, the decline in cell abundance corresponding to a decrease in water transparency during PrM shows the importance of water transparency for this group which is supported by the positive correlation of *SYN-PEII* with water transparency from 2 d in reverse time and at zero time lag.

SYN-PC was observed throughout the study period in low saline as well as in high saline waters. Studies carried out in the same estuary as well as others have shown that this group is dominant in the upper estuary characterized by lower salinities [16,17,33]. It is currently unclear what drives this apparent salinity pattern but may be a physiological adaptation to lower salinity, or other variables expected to covary with salinity in estuarine environments such as nutrients and light [42]. Transient abundance peaks during the break in precipitation periods in MON is supported by the positive correlation with temperature and solar radiation and no relation with nutrients. However, cross correlation results showed that this group is negatively related with salinity in forward time and positively related in reverse time which suggests its dominance at intermediate salinities. This is also supported by the negative relation with water transparency. Earlier observations along

this estuary has shown the dominance of this group in intermediate saline waters [17]. However, an abundance peak of this group during PrM, when the salinity is high, suggests that salinity may not be the only factor controlling the distribution of this group. A negative correlation with water transparency suggests that this group can grow in waters with low transparency as shown in earlier studies that this group is known to prefer red wavelengths of the light spectrum [43]. This peak also corresponded with a peak in nitrate concentration and this positive response to an ephemeral nitrate peak suggests that *SYN-PC* growth is positively influenced by NO_3^- availability which was probably introduced into the surface waters by benthic resuspension as there was corresponding decrease in water transparency. This was supported by a positive relation of $< 3 \mu\text{m chl } a$ with NO_3^- . *SYN-PC* abundance decreased 2 d after increase in water transparency and increased at zero time lag. This could imply that *SYN-PC* distribution is governed by the light spectrum which is controlled by the turbidity i.e., if turbidity is high, red light dominates and also nutrients are available due to resuspension or influx from freshwater. These transient increases are usually missed in monthly samplings which portray a different picture of the distribution of this group. Existence of salinity specific strains is also a possibility [44].

PRO-like cells were higher in waters with lower salinities and lower transparency during MON. During the PrM, *PRO*-like cells were higher when the water transparency was low along with lower solar radiation. This coincided with the period of increased nutrient concentration. However it did not show any significant relationship with nutrients like *SYN-PC* which suggests that the increase in abundance was not so high. PEUK cell abundance ranged up to 1.0×10^4 cells mL^{-1} which was slightly lower than that reported in the coastal surface waters of Western Arabian Sea (1.7×10^4 cells mL^{-1}) [14] where even during intense monsoonal forcing, picoeukaryotic algae appeared to account for a large portion of primary production. Similarly in the present study, comparatively higher abundance was observed during MON. Positive correlation with salinity and water transparency along with a negative correlation with NH_4^+ could imply its utilisation by PEUK. This could also explain its lower abundance during the PM and PrM when the environmental conditions were stable but nutrient concentrations were low. Although a significant relation was not observed between PEUK and nutrients, abundance peaks in PEUK followed peaks in NH_4^+ concentrations which could signify a lagged response.

Contribution of picophytoplankton to total photosynthetic biomass

Comparison of data from the Atlantic, Pacific and Indian Oceans showed that the contribution by PP to total carbon production was considerably higher in oligotrophic open oceans (50-80%) than in meso and eutrophic coastal marine waters (2-25%) [45]. In the western Arabian Sea, PP comprised up to 35% in the diatom dominated coastal zone [14]. In waters between 5 and 23 salinity of a sub-tropical estuary, phytoplankton biomass was primarily (50%) composed of $< 5 \mu\text{m}$ cells and results from this study supported the idea that a microbial food web characterizes mass and energy flow through the planktonic food web in estuaries [46]. In the Dona Paula Bay, PP contribution to total photosynthetic biomass was substantial (up to 49%) throughout the year.

Observations in other estuarine and coastal waters have shown a significant contribution of eukaryotes to PP biomass [47]. In the Western Arabian Sea, PEUK were particularly abundant and disproportionately productive in coastal marine systems, even during intense monsoonal forcing [14]. These observations are not in par with the results obtained from the Dona Paula Bay. This disparity could be because of the presence of *PRO*-like cells and *SYN*-PC groups in our observation which were not encountered or overlooked in the earlier observations. This aspect needs to be considered in future studies since it can underestimate the importance of PP in coastal ecosystems.

In the warmer tropical systems a strong interactive network of producers and consumers is maintained throughout the year [48]. Protistan grazers in pelagic food webs are almost always capable of preventing the formation of high biomass blooms of PP [49]. Increased loss rates through grazing could be responsible for the lowered contribution of PP in warm productive waters whereas their dominance in warm, oligotrophic waters is attributable to differential capacity to acquire nutrients [40]. The high frequency sampling in the present study showed that PP abundance are short lived which could be due to high grazing pressure as a result of which the PP community abundance remains stable as reported from the samplings conducted at low frequency [16,17]. This aspect needs to be taken into consideration in future studies with high frequency samplings which will improve our understanding of the role of PP dynamics in the microbial food web of different ecosystems.

Conclusions

High resolution sampling showed that the PP community structure at Dona Paula Bay is shaped by the direct effects of physical processes (freshwater influx, rainfall intensity, breaks in MON, tides) as well as their indirect effects on salinity, water transparency, solar radiation and nutrient availability. Through this time series observations, growth responses driven by natural enrichment transients during the temporal expressions of complex processes could be captured. This study showed that the coastal PP community in a MON influenced tropical estuary responded in par with rest of the autotrophic community during favorable transients thus supporting the “rising tide” hypothesis proposed for the oligotrophic open-oceanic regions. The $< 3 \mu\text{m}$ chl *a* biomass during non-MON was almost similar to that observed during the MON precipitation breaks which suggests that the environmental factors leading to a stable water column exert a greater positive influence on the growth of PP than the nutrient concentrations as compared to the higher phytoplankton which require high nutrient concentrations for their growth PP. PP, especially *SYN* containing PC and PE could be useful tracers of the coastal hydrography such as freshwater influx during monsoon and tidal influence during the non-monsoon, respectively. Their contribution to the total photosynthetic biomass was also significant. These observations suggest that the microbial food web is active throughout the year and can play an important role in the food web dynamics of coastal regions.

Acknowledgements

The authors are grateful to Dr. S.W.A. Naqvi, Director, and Dr. A. C. Anil, Chief scientist, CSIR-National Institute of Oceanography, for their support and encouragement. The authors thank the anonymous reviewers for their valuable suggestions which helped to improve the manuscript. This is NIO contribution #.

References

1. Sosik HM, Olson RJ, Neubert MG, Shalapyonok A (2003) Growth rates of coastal phytoplankton from time-series measurements with a submersible flow cytometer. *Limnol Oceanogr* 48:1756-1765
2. Lefort T, Gasol JM (2013) Short-time scale coupling of picoplankton community structure and single-cell heterotrophic activity in winter in coastal NW Mediterranean Sea waters. *J Plank Res* 36:243–258
3. Torreton JP, Rochelle-Newall E, Pringault O, Jacquet S, Faure V, Briand E (2010) Variability of primary and bacterial production in a coral reef lagoon (New Caledonia). *Mar Poll Bull* 61:335–348
4. Harris GP (1984) Phytoplankton productivity and growth measurements: past, present and future. *J Plank Res* 6: 219–237
5. Vaultot D, Marie D (1999) Diel variability of photosynthetic picoplankton in the equatorial Pacific. *J Geophys Res* 104:3297-3310
6. Williams PJJ, Morris PJ, Karl DM (2004) Net community production and metabolic balance at the oligotrophic ocean site, station ALOHA. *Deep-Sea Res I* 51:1563–1578
7. Jacquet S, Prieur L, Jacquet C, Lennon JF, Vaultot D (2002) Short-timescale variability of picophytoplankton abundance and cellular parameters in surface waters of the Alboran Sea (western Mediterranean). *J Plank Res* 24:635–651
8. Liu H, Campbell L, Landry MR, Nolla HA, Brown SL, Constantinou J (1998) *Prochlorococcus* and *Synechococcus* growth rates and contributions to production in the Arabian Sea during the 1995 Southwest and Northeast Monsoons. *Deep-Sea Res II* 45:2327–2352
9. Shetye SR, Murty CS (1987) Seasonal variation of the salinity in the Zuari estuary, Goa, India. *Proceedings of Indian Academy of Sciences (Earth and Planetary Sciences)* 96:249–257
10. Shetye SR, Shankar D, Neetu S, Suprit K, Michael GS, Chandramohan P (2007) The environment that conditions the Mandovi and Zuari estuaries. In: Shetye SR, Dileepkumar M, Shankar D (eds), *The Mandovi and Zuari estuaries*. National Institute of Oceanography, Dona Paula, Goa
11. Patil JS, Anil AC (2011) Variations in phytoplankton community in a monsoon-influenced tropical estuary. *Environ Monit Assess* 182:291–300
12. Pednekar S, Matondkar SGP, Gomes H, Goes J, Parab S, Kerkar V (2011) Fine-scale responses of phytoplankton to freshwater influx in a tropical monsoonal estuary following the onset of southwest monsoon. *J Earth Syst Sci* 120:545–556
13. Campbell L, Landry MR, Constantinou J, Nolla HA, Brown SL, Liu H, Caron DA (1998) Response of microbial community structure to environmental forcing in the Arabian Sea. *Deep Sea Res II* 45:2301–2325
14. Brown SL, Landry MR, Barber RT, Campbell L, Garrison DL, Gowing MM (1999) Picophytoplankton dynamics and production in the Arabian Sea during the 1995 Southwest Monsoon. *Deep Sea Res II* 46: 1745–1768

15. Mitbavkar S, Anil AC (2011) Tiniest primary producers in the marine environment: An appraisal from the context of waters around India. *Curr Sci* 100:986–988
16. Mitbavkar S, Rajaneesh KM, Anil AC, Sundar D (2012) Picophytoplankton community in a tropical estuary: Detection of *Prochlorococcus*-like populations. *Estuar Coast Shelf Sci* 107:159–164
17. Rajaneesh KM, Mitbavkar S (2013) Factors controlling the temporal and spatial variations in *Synechococcus* abundance in a monsoonal estuary. *Mar Environ Res* 92:133-143
18. Binder BJ, Chisholm SW, Olson RJ, Frankel SL, Worden AZ (1996) Dynamics of picophytoplankton, ultraphytoplankton and bacteria in the central equatorial Pacific. *Deep-Sea Res II* 43:907-931
19. Teno'rio MMB, Le Borgne R, Rodier M, Neveux J (2005) The impact of terrigenous inputs on the Bay of Ouinne' (New Caledonia) phytoplankton communities: A spectrofluorometric and microscopic approach. *Estuar Coast Shelf Sci* 64:531–545
20. Qasim SZ, Sengupta R (1981) Environmental characteristics of the Mandovi–Zuari estuarine system in Goa. *Estuar Coast Shelf Sci* 13:557–578
21. Sundar D, Shetye SR (2005) Tides in the Mandovi and Zuari estuaries, Goa, west coast of India. *J Earth Syst Sci* 114:493–503
22. Chandramohan P, Jaya Kumar S, Kumar S, Ilangoan D (1997) Fine particle deposition at Vainguinim Tourist beach, Goa, India. *J Coast Res* 14:1074–1081
23. Parsons TR, Maita Y, Lalli CM (1984) *A Manual of Chemical and Biological Seawater Analysis*. Pergamon, New York
24. Worden AZ, Nolan JK, Palenik B (2004) Assessing the dynamics and ecology of marine picophytoplankton: The importance of the eukaryotic component. *Limnol Oceanogr* 49:168-179
25. Baudoux AC, Veldhuis MJW, Witte HJ, Brussaard PD (2007) Viruses as mortality agents of picophytoplankton in the deep chlorophyll maximum layer during IRONAGES III. *Limnol Oceanogr* 52:2519–2529
26. Pennock JR (1985) Chlorophyll distribution in the Delaware estuary: regulation by light-limitation. *Estuar Coastal Shelf Sci* 21:711–725
27. Cote B, Platt T (1983) Day-to-day variations in the spring-summer photosynthetic parameters of coastal marine phytoplankton. *Limnol Oceanogr* 28:320–344
28. Lantoiné F, Neveux J (1997) Spatial and seasonal variations in abundance and spectral characteristics of phycoerythrins in the tropical northeastern Atlantic Ocean. *Deep-Sea Res* 44:223-246
29. Palenik B (2001) Chromatic adaptation in marine *Synechococcus* strains. *Appl Environ Microbiol* 67:991-994
30. Campbell L, Carpenter EJ (1987) Characterization phycoerythrin-containing *Synechococcus* spp. populations by immunofluorescence. *J Plank Res* 9:1167–1181
31. Callieri C, Amicucci E, Bertoni R, Voros L (1996) Fluorometric characterization of two picocyanobacteria strains from lakes of different underwater light quality. *Int Rev Hydrobiol* 81:13–23
32. Moser M, Callieri C, Weisse T (2009) Photosynthetic and growth response of freshwater picocyanobacteria are strain-specific and sensitive to photoacclimation. *J Plank Res* 31:349–357

33. Ray RT, Haas LW, Sieracki ME (1989) Autotrophic picoplankton dynamics in a Chesapeake Bay sub-estuary. *Mar Ecol Prog Ser* 52:273–285
34. Shalapyonok A, Olson RJ, Shalapyonok LS (2001) Arabian Sea phytoplankton during Southwest and Northeast Monsoons 1995: composition, size structure and biomass from individual cell properties measured by flow cytometry. *Deep-Sea Res II* 48:1231-1261
35. Partensky F, Hess WR, Vault D (1999) *Prochlorococcus*, a marine photosynthetic prokaryote of global significance. *Microbiol Mol Biol Rev* 63:106–127
36. Paerl HW, Valdes LM, Peirls BL, Adolf JE, Harding LW Jr (2006) Anthropogenic and climatic influences on the eutrophication of large estuarine ecosystems. *Limnol Oceanogr* 51: 448-462
37. SubhaAnand S, S. Sardesai, C. Muthukumar, K.R. Mangalaa, D. Sundar, S.G. Parab, M. Dileep Kumar (2014) Intra- and inter-seasonal variability of nutrients in a tropical monsoonal estuary (Zuari, India). *Continental Shelf Research* 82: 9-30
38. Baek SH, Shimode S, Kim H, Han M, Kikuchi T (2009) Strong bottom-up effects on phytoplankton community caused by a rainfall during spring and summer in Sagami Bay, Japan. *J Mar Syst* 75: 253-264
39. Morse RE, Mulholland MR, Egerton TA, Marshall HG (2014) Phytoplankton and nutrient dynamics in a tidally dominated eutrophic estuary: daily variability and controls on bloom formation. *Mar Ecol Prog Ser* 503: 59-74
40. Agawin NSR, Duarte CM, Agusti S (2000) Nutrient and temperature control of the contribution of picoplankton to phytoplankton biomass and production. *Limnol Oceanogr* 45:591–600
41. Wong MW, Townsend DW (1999) Phytoplankton and hydrography of the Kennebec estuary, Maine, USA. *Mar Ecol Prog Ser* 178:133–144
42. Murrell MC, Lores EM (2004) Phytoplankton and zooplankton seasonal dynamics in a subtropical estuary: importance of cyanobacteria. *J Plank Res* 26:371–382
43. Stomp M, Huisman J, Jongh F, Veraart AJ, Gerla D, Rijkebeer M, Ibelings BW (2004) Adaptive divergence in pigment composition promotes phytoplankton diversity. *Nature* 432: 104-107
44. Waterbury JB, Rippka R (1989) Order Chroococcales. In: *Bergey's manual of systematic bacteriology*, vol 3, Staley JT, Bryant MP, Pfennig N and Holt JG (ed) Williams and Wilkins, Baltimore, pp 1729-1746
45. Bell T, Kalff J (2001) The contribution of picophytoplankton in marine and freshwater systems of different trophic status and depth. *Limnol Oceanogr* 46:1243–1248
46. Putland JN, Iverson RL (2007) Phytoplankton biomass in a subtropical estuary: Distribution, size composition, and carbon:chlorophyll ratios. *Estuar Coasts* 30:878–885
47. Thomsen HA (1986) A survey of the smallest eukaryotic organisms of the marine phytoplankton. In: Platt T., Li W.K. (Eds), *Photosynthetic picoplankton*. *Canad J Fish and Aquat Sci*, Department of Fisheries and Oceans, Ottawa: 121–158
48. Linacre LP, Landry MR, Lara-Lara JR, Hernandez-Ayon JM, Carmen BG (2010) Picoplankton dynamics during contrasting seasonal oceanographic conditions at a coastal upwelling station off Northern Baja California, Mexico. *J Plank Res* 32:539–557
49. Barber RT, Hiscock MR (2006) A rising tide lifts all phytoplankton: Growth response of other phytoplankton taxa in diatom-dominated blooms. *Glob Biogeochem Cyc* 20:1–12

LEGEND FOR FIGURES

Fig. 1. Location of study area

Fig. 2. Dot plot of flow cytometric analysis showing picophytoplankton populations.

Fig. 3. Daily variations in the solar radiation (A), rainfall (B), secchi disk depth (C), temperature (D) and salinity (E) at the Dona Paula Bay

Fig. 4. Temporal variations in the nitrate (NO₃-N; A), nitrite (NO₂-N; B), ammonia (NH₄-N; C), phosphate (PO₄-P; D) and silicate (SiO₄; E) at the Dona Paula Bay

Fig. 5. Daily variations in total chlorophyll concentration (A), total chlorophyll fluorescence (B), < 3 μm chlorophyll fluorescence (C) and contribution of < 3 μm fraction to total chlorophyll fluorescence (D) at the Dona Paula Bay

Fig. 6. Daily variations in the picophytoplankton abundance. *Synechococcus*-PEI (A), *Synechococcus*-PEII (B), *Synechococcus*-PC (C), *Prochlorococcus*-like cells (D), picoeukaryotes (E) and total picophytoplankton (F) at the Dona Paula Bay

Fig. 7. Cross-correlation function between (A) environmental variables (rainfall versus solar radiation, temperature and salinity and salinity versus secchi disk depth) and between biological and environmental variables (water temperature, salinity, secchi disk depth and solar radiation) for monsoon. Biological variables used were total chlorophyll fluorescence (B), < 3 μm chlorophyll (C), *Synechococcus*-PEI (D), *Synechococcus*-PEII (E), *Synechococcus*-PC (F), *Prochlorococcus*-like cells (G) and picoeukaryotes (H). In all the plots a 7 d forward and reverse time lag is shown along the x-axis with day 0 being the present (no time lag). Along the y-axis the correlation coefficient at each time lag is shown with 95% CI for correlations (shown as shaded region). The data points outside the shaded region were significant.

Fig. 8. Cross-correlation function between (A) environmental variables (salinity versus secchi disk depth) and between biological and environmental variables (water temperature, salinity, secchi disk depth and solar radiation) for post-monsoon i.e. December 2008. Biological variables used were total chlorophyll fluorescence (B), < 3 μm chlorophyll (C), *Synechococcus*-PEI (D), *Synechococcus*-PEII (E), *Synechococcus*-PC (F), *Prochlorococcus*-like cells (G) and picoeukaryotes (H). In all the plots a 7 d forward and reverse time lag is shown along the x-axis with day 0 being the present (no time lag). Along the y-axis the correlation coefficient at each time lag is shown with 95% CI for correlations (shown as shaded region). The data points outside the shaded region were significant.

Fig. 9. Cross-correlation function between (A) environmental variables (salinity versus secchi disk depth) as well as between biological and environmental variables (water temperature, salinity, secchi disk depth and solar radiation) for pre-monsoon i.e. April 2009. Biological variables used were total chlorophyll fluorescence (B), < 3 μm chlorophyll (C), *Synechococcus*-PEI (D), *Synechococcus*-PEII (E), *Synechococcus*-PC (F), *Prochlorococcus*-like (G) and Picoeukaryotes (H). In all the plots a 7 d forward and reverse time lag is shown along the x-axis with day 0 being the present (no time lag). Along the y-axis the correlation coefficient at each time lag is shown with 95% CI for correlations (shown as shaded region). The data points outside the shaded region were significant.

Fig. 10. Tidal amplitude and *Synechococcus*-PEII abundance in the Dona Paula Bay during the study period

Fig. 11. Ratio of *Synechococcus*-PC and *Synechococcus*-PE abundance in the Dona Paula Bay during the study period

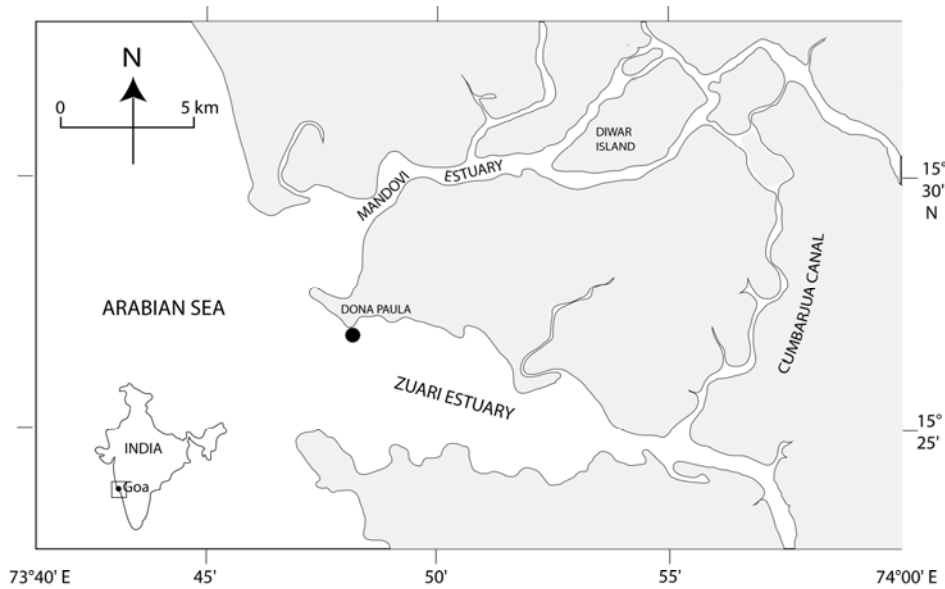


Fig. 1

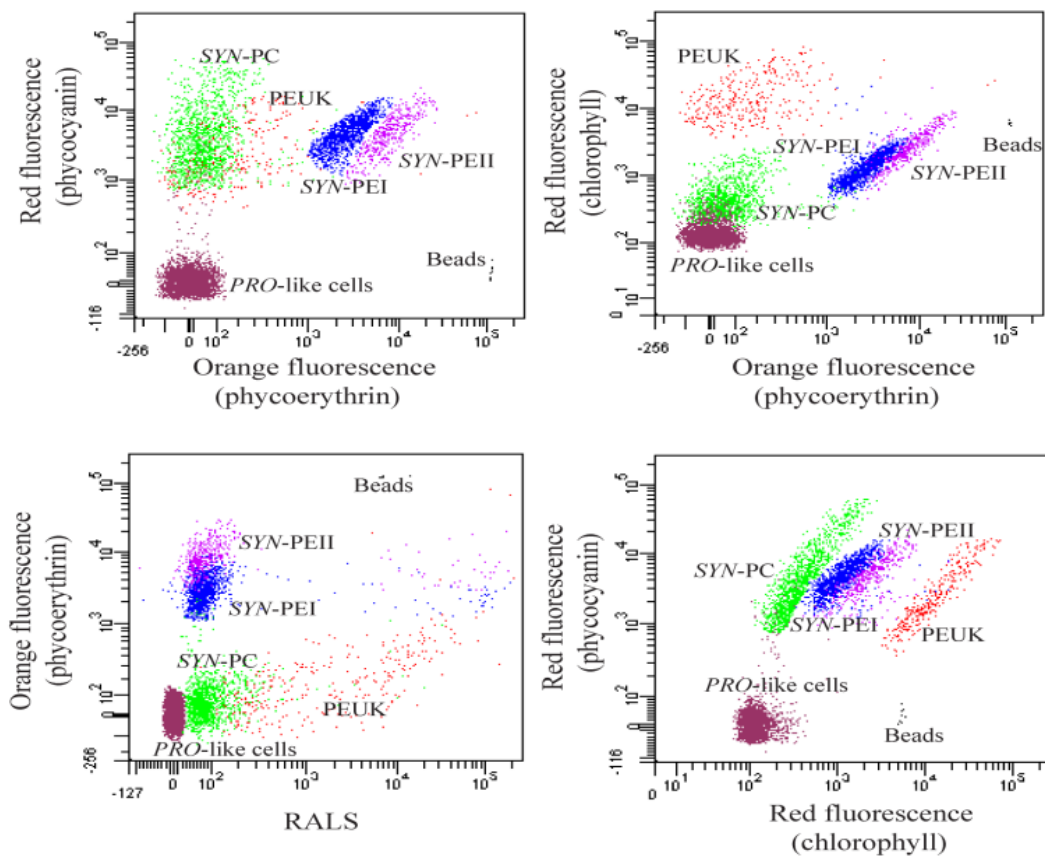


Fig. 2

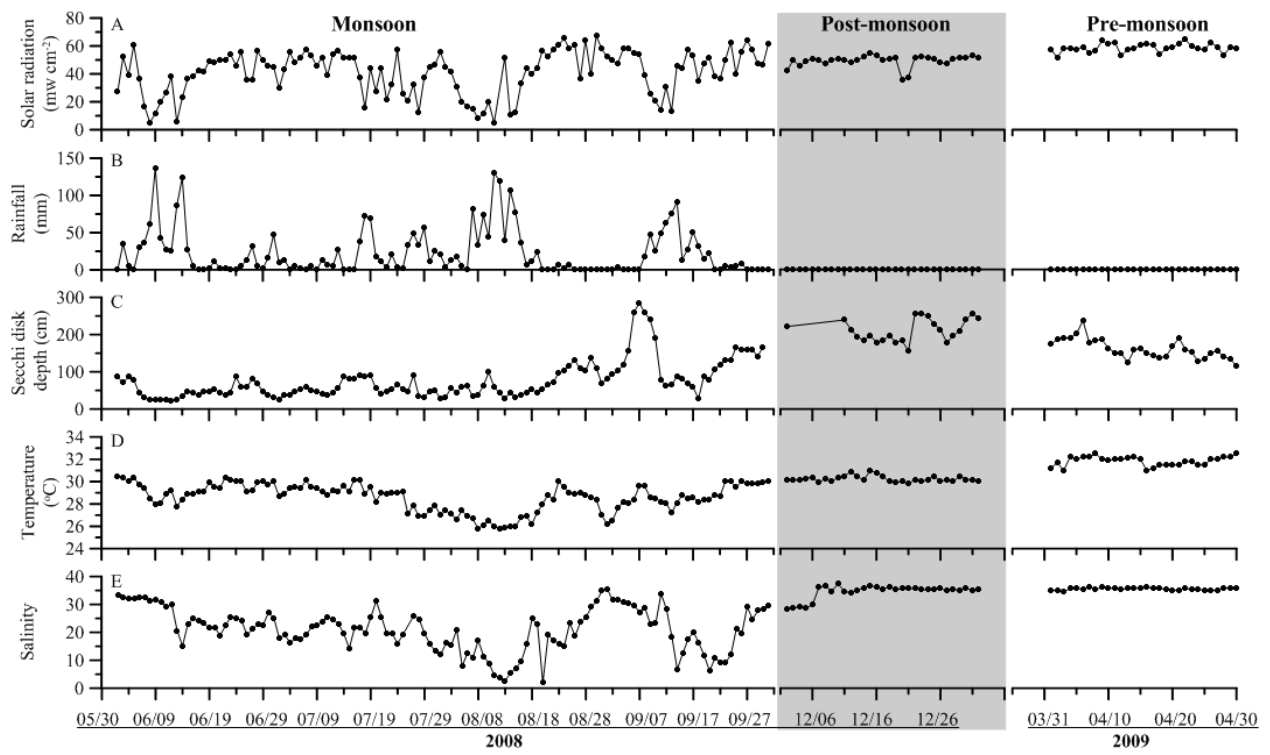


Fig. 3

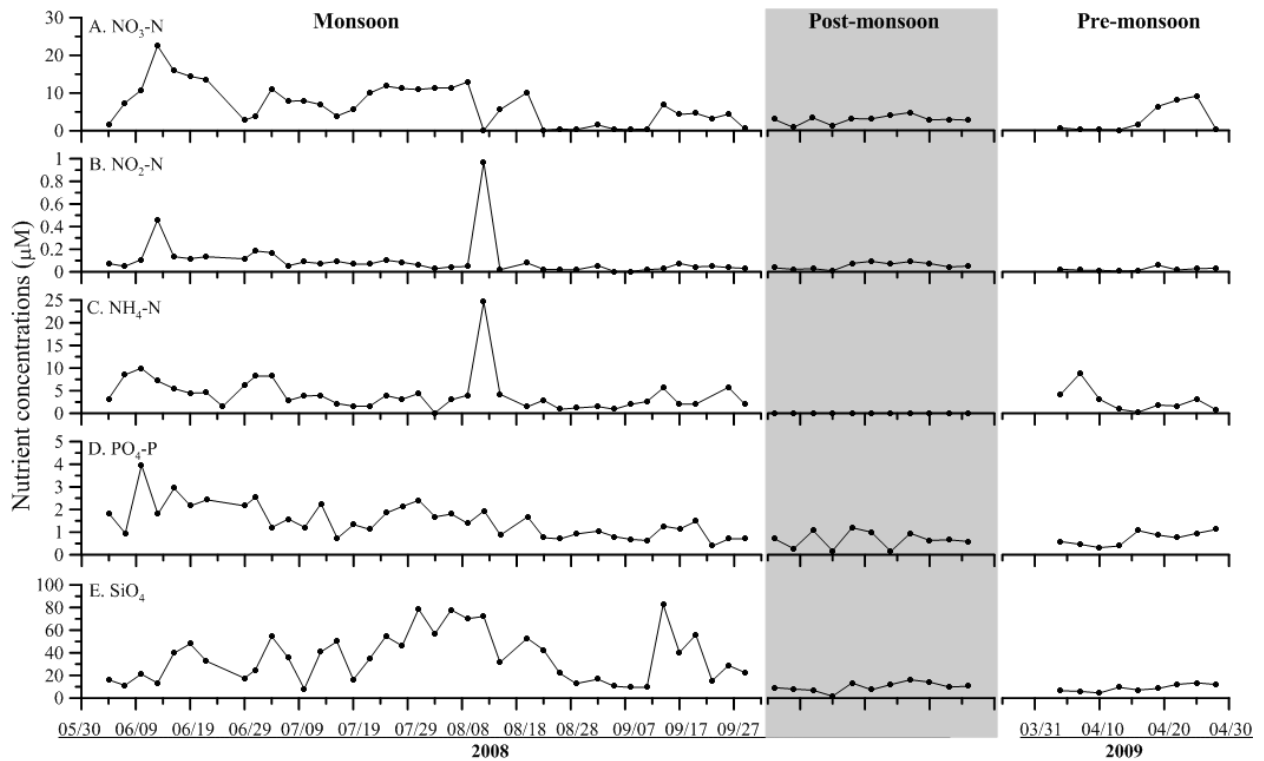


Fig. 4

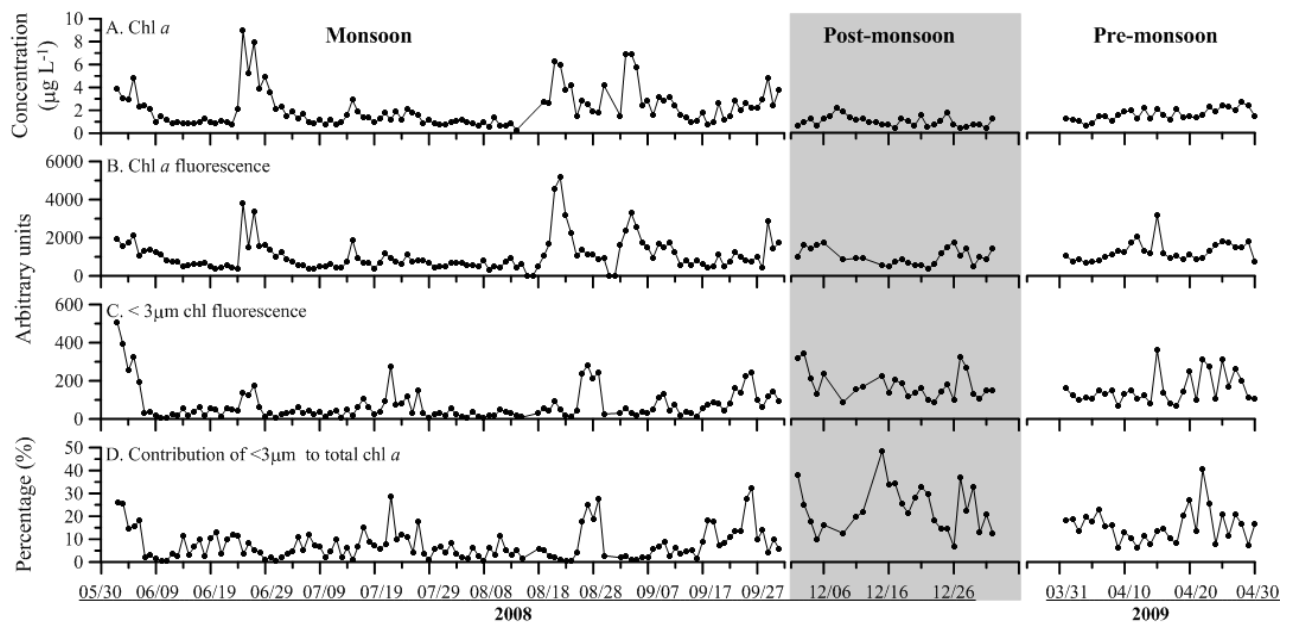


Fig. 5

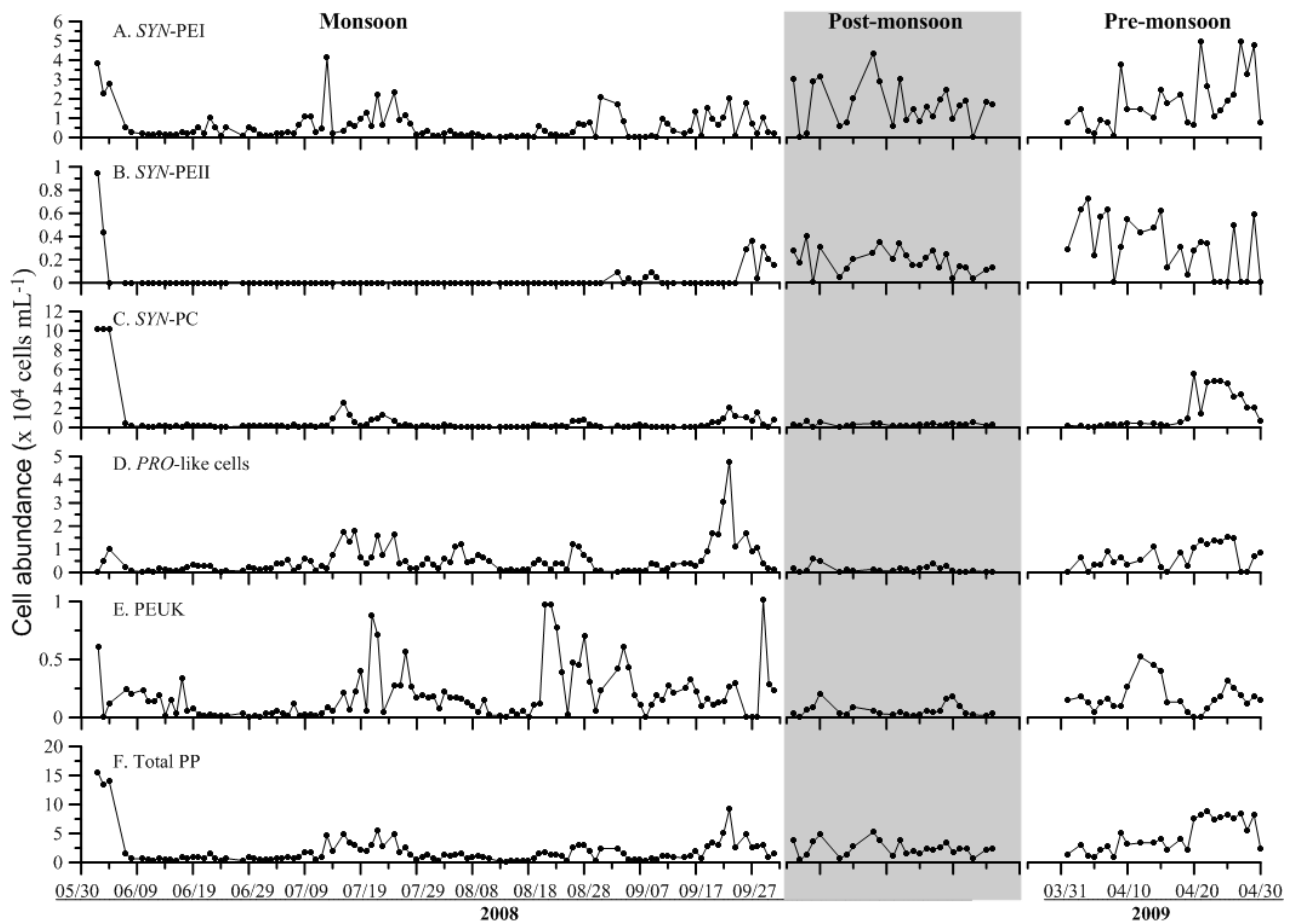


Fig. 6

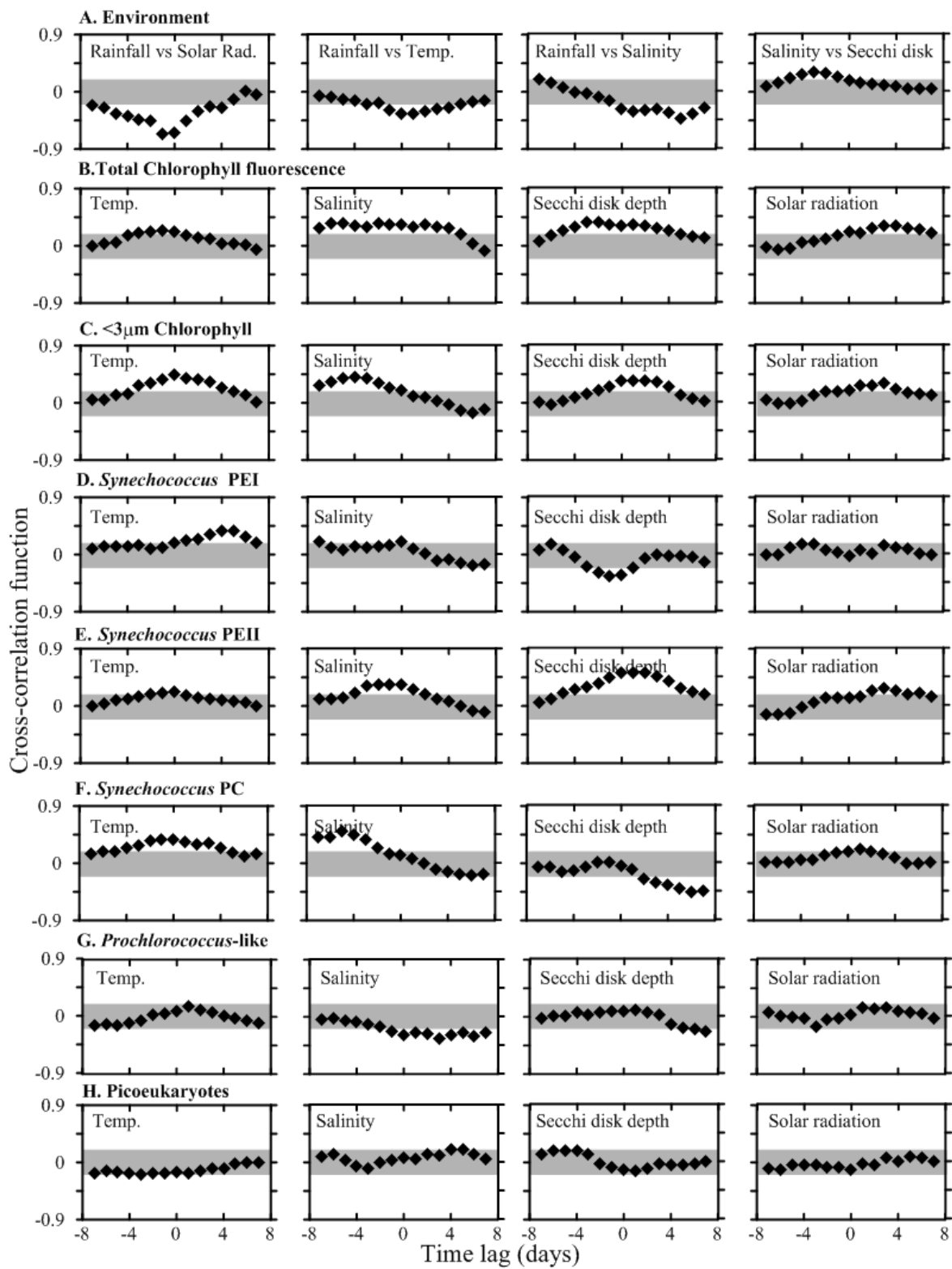


Fig. 7

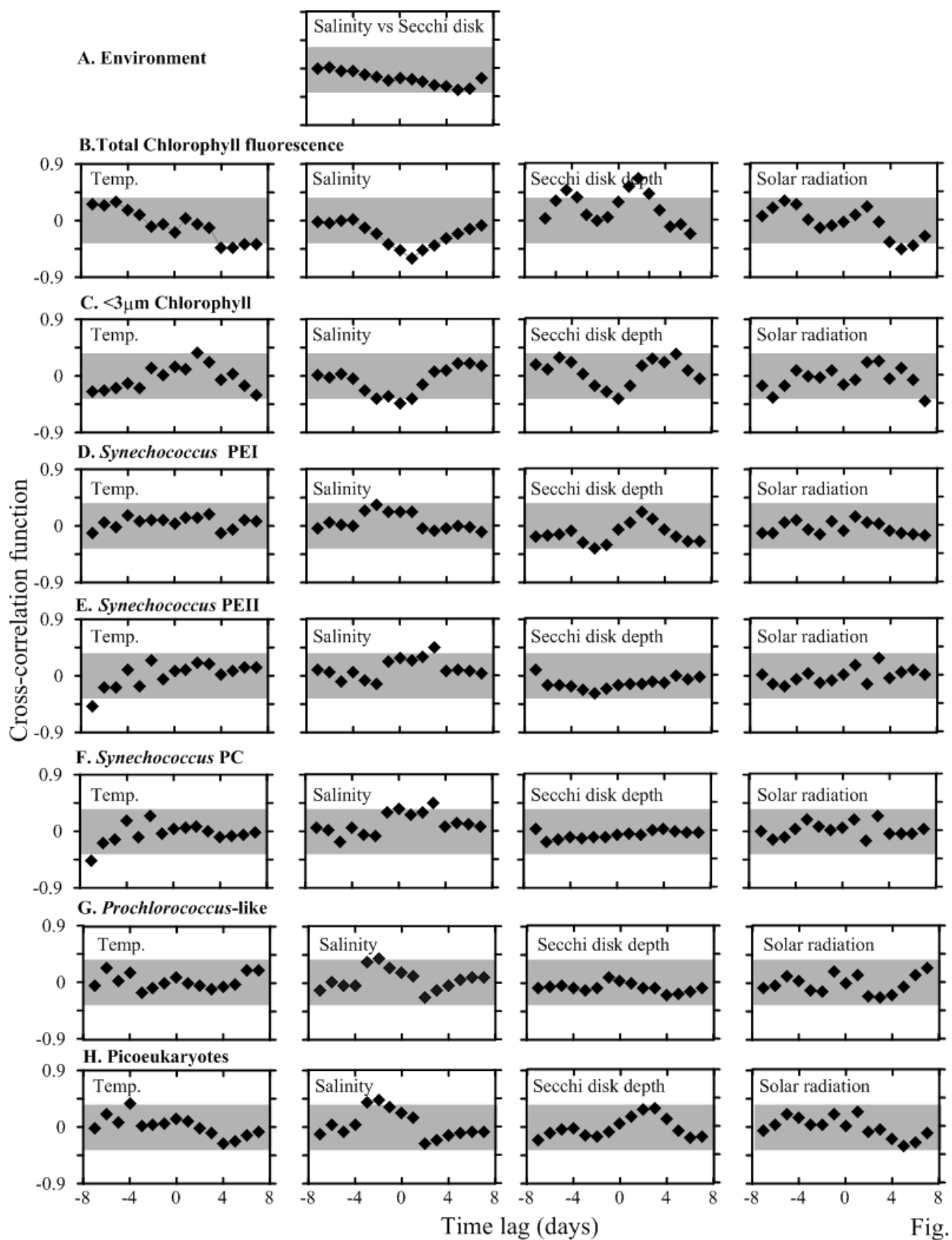


Fig. 8

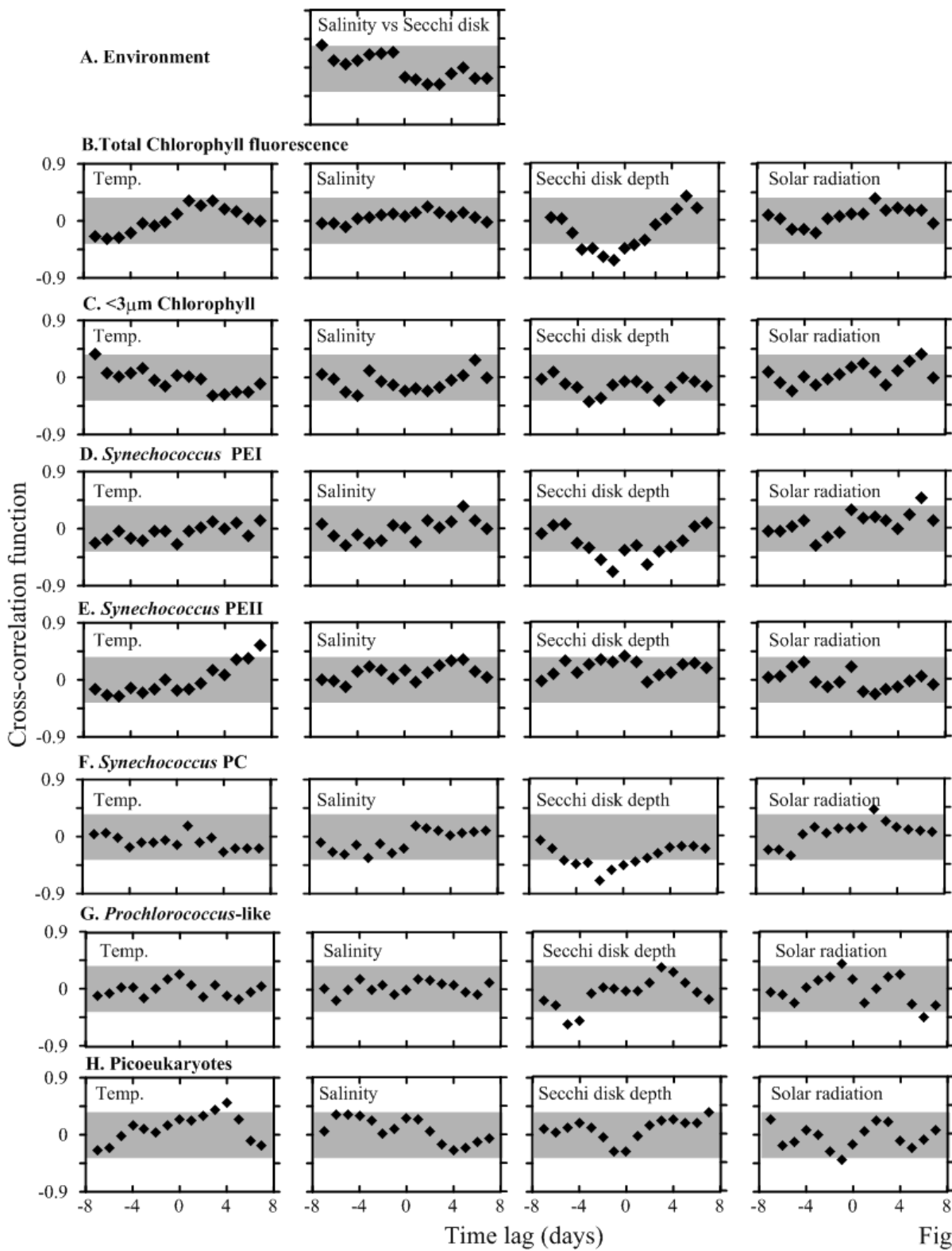


Fig. 9

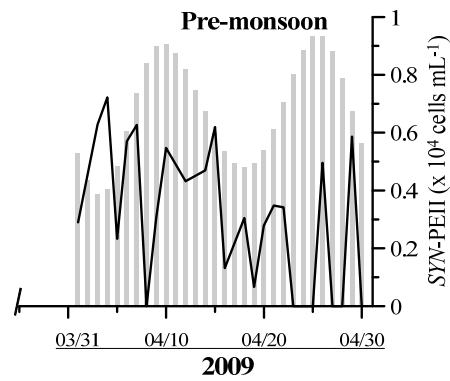
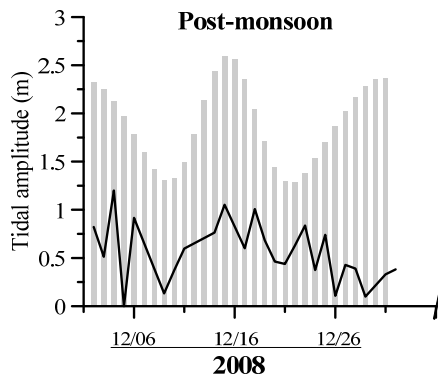
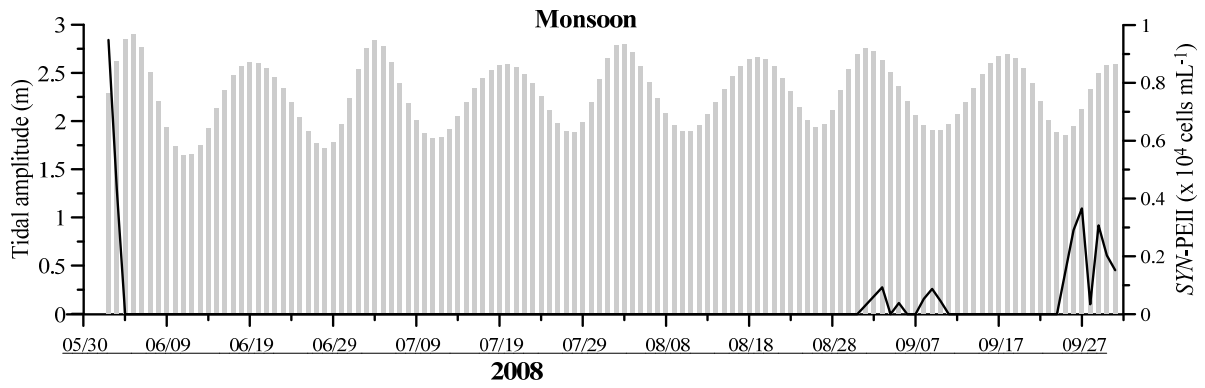


Fig. 10

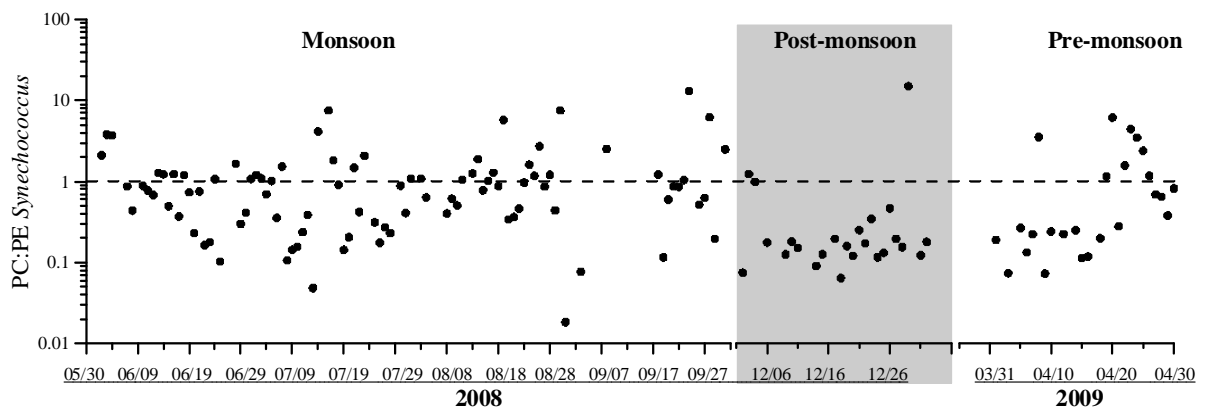


Fig. 11